Dalton Transactions

Accepted Manuscript

ROYAL SOCIETY OF CHEMISTRY

www.rsc.org/dalton

Journal Name

RSCPublishing

ARTICLE

AIE-Active Organoboron Complexes with Highly Efficient Solid-State Luminescence and Their Application as Gas Sensitive Materials

Cite this: DOI: 10.1039/xoxxoooooox

Received ooth January 2012,
Accepted ooth January 2012

DOI: 10.1039/xoxxoooooox

www.rsc.org/

Shuwen Gong,[†,a] Qingsong Liu,[†,a] Xiaoqing Wang,*[,a,b] Bo Xia,[a] Zhipeng Liu,*[,a] and Weijiang He*[,c]

Complexation of a boron atom with two of benzothiazole-enolate-based bidentate ligands successfully gave rise to corresponding BF_2-/BPh_2-chelated complexes (**3**–**6**), which could be considered as novel AIE-active organoboron luminophores. These new luminophores exhibited aggregation-induced emission, and large Stokes shift in solution. In solid-state, compounds **3**–**6** exhibited intense emission with high quantum yields of 0.14–0.43. The photophysical properties and AIE characteristics of these compounds were rationalized through X-ray crystal analysis and theoretical calculations. In addition, compounds **4** and **6** were capable of sensing acidic gas by reversible changes of emission, which may potentially serve as solid-state luminescent sensors for acidic vapors.

Introduction

Boron dipyrromethenes (BODIPYs) are an outstanding class of organic dye molecules that have been widely applied in the field of luminescent sensing/imaging, biological labelling, and dye-sensitized solar cells.[1,2] The success of BODIPYs in these applications is attributed to their excellent properties (e.g. high molar absorption coefficients and luminescence quantum yields, and tunable emission from visible light to near infrare) in their diluted solution state.[2] Unfortunately, despite their intense luminescence in diluted solution, BODIPYs show very weak emission in their aggregated states due to "aggregation-caused emission quenching (ACQ)". The ACQ of BODIPYs has greatly limited the practical applications of BODIPYs in the field of materials science.[2c,3] A prominent strategy to avoid the ACQ of BODIPYs is to decorate the periphery of the BODIPY core with bulky groups.[4] Apart from the dipyrrin framework, several groups have focused their attention on developing newer analogues of BODIPYs with unsymmetrical structures to achieve solid-state luminescence properties. Indeed, several new BODIPYs with solid-state emission from moderate to high have been reported.[2c,5]

In the course of our efforts in developing solid-state emissive BODIPYs, we are interested in the boron complexes with aggregation-induced emission (AIE).[6,7] Recently, we reported that desymmetrized *N*,*N*-bidentate-ligand-based boron complexes having propeller-shaped structure show interesting luminescence properties such as AIE and high solid-state emission.[7a,b,c] In light of these results, we realized that the unsymmetry and propeller-shaped structure of boron complexes in solid-state might lead to AIE and intense solid-state emission. In this study, we report the synthesis and luminescence properties of benzothiazole-enolate-ligand-based boron complexes (**3**–**6**) with asymmetry and propeller-shaped structure, which showed AIE effect and intense solid-state emission.

Results and discussion

Design and synthesis. Compounds **3**–**6** are analogues of BODIPYs derived from unsymmetrical *N^O*–bidentate ligands. The three-ring-fused π-conjugated skeleton (**A** and **B**) of compounds **3**–**6** was constructed via the boron coordination of the benzothiazole-enolate derived ligands. Two phenyl groups (**C** and **D**) were decorated to ring B to form a propeller-shaped structure. Compounds **3**–**6** were expected to display large Stokes shift and AIE due to their unsymmetrical nature and the restricted intramolecular rotation of phenyl groups **C** and **D**.

The synthetic route for compounds **3**–**6** is illustrated in scheme 1. The reaction of 2-benzylbenzothiazole with ethyl benzoate or ethyl 4-(dimethylamino) benzoate in presence of sodium hydride in tetrahydrofuran (THF) gave *N^O*–bidentate ligands **1** and **2**. Compound **1** consists of a tautomeric mixture of iminoketone (**1a**) and iminoenol (**1b**), and the ratio of **1a** and **1b** was 1:2 in $CDCl_3$. Interestingly, only iminoenol form was observed for compound **2** in $CDCl_3$, suggesting that iminoketone form of compound 2 was stabilized by *N*,*N*-dimethylamino group. By reacting of compounds **1** and **2** with boron trifluoride diethyl ether complex in the presence of 1,8-diazabicyclo[5.4.0]undec-7-ene (DBU) in toluene gave the BF_2 complexes, **3** and **4**. The reaction of compounds **1** and **2** with triphenylborane in toluene gave corresponding BPh_2 complexes,

5 and **6**. The structures of compounds **3**–**6** were confirmed by ^{1}H, ^{13}C NMR, HRMS, and X-ray crystallography.

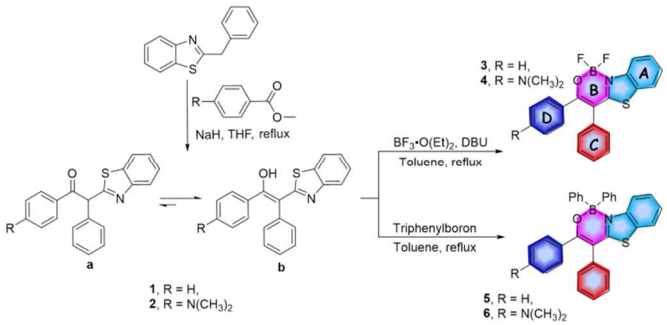

Scheme 1. Synthetic routes for compounds **3**–**6**.

Photophysical properties. The photophysical properties of compounds **3**–**6** were measured in solution and in solid-state. The related data are summarized in Table 1. In THF, compound **3** showed the maximum absorption wavelength (λ_{abs}) at 372 nm (ε = 43000 $M^{-1}cm^{-1}$), which can be assigned to the π–π^* transition band (Fig. 1a). Compound **4** showed λ_{abs} at 443 nm (ε = 49000 $M^{-1}cm^{-1}$), which can be assigned to the charge transfer (CT) transition band. Compounds **3** and **4** showed weak luminescence in THF with the maximum emission wavelength (λ_{em}) at 449 nm (Φ_f<0.01) and 512 nm (Φ_f<0.01), respectively (Fig. 1b). Compared to compound **3**, the large red-shifted absorption (71 nm) and emission band (63 nm) of compound **4** can be ascribed to the *N*,*N*-dimethylamino group in **D** ring caused CT enhancement. Compound **5** exhibited large red-shifted absorption (32 nm) and emission (24 nm) bands and lower molar absorption coefficients compared to compound **3**, with λ_{abs} and λ_{em} at 404 nm (ε = 35000 $M^{-1}cm^{-1}$) and 473 nm (Φ_f<0.01), respectively (Fig. 1). This red-shift of λ_{abs} and λ_{em} and a decrease in ε of compound **5** may be due to the molecular bending of compound **5** caused by the introduction of bulky phenyl groups at the boron atom.[7a] Interestingly, compound **6** showed almost the same λ_{abs} (444 nm, ε = 35000 $M^{-1}cm^{-1}$) and λ_{em} (510 nm, Φ_f <0.01) compared to compound **4**, suggesting CT progress played more important role than molecular bending effect induced by phenyl groups at boron atom. Moreover, the Stokes shifts of compounds **3**–**6** are in the range of 3000-4600 cm^{-1}, which are larger than some of *N*^*O*– and *N*^*N*–bidentate ligand-based BODIPYs which were reported in ref. 5 (e.g. ref. 5f,n with shifts ranging from 430–9200 cm^{-1} and ref. 5c,h,i, with shifts ranging from 452–5600 cm^{-1}).

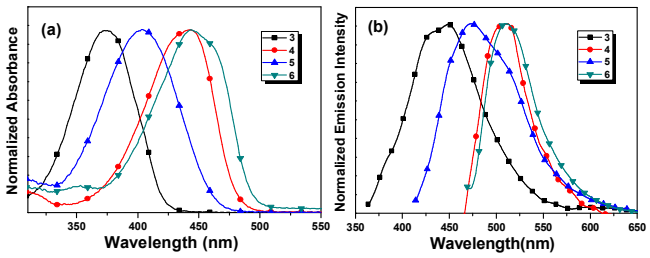

Fig. 1. Normalized absorption (a) and emission spectra (b) of compounds **3**–**6** in THF (10 μM).

The absorption and emission properties of compounds **3**–**6** in different solvents were examined (Fig. S1 and 2). The λ_{abs} of compounds **3**–**6** were less affected by solvent polarity and viscosity. While the ε of compounds **3**–**6** were varied in different solvents. As expected, compounds **3**–**6** showed very weak emission intensity in low-viscosity solvents along with very low Φ_f (<0.01) due to the intramolecular rotation induced nonradiative process. While in high-viscosity solvents such as glycerol, the emission intensity of these compounds was dramatically enhanced, with Φ_f of 0.12 for compound **3**, 0.26 for compound **4**, 0.29 for compound **5**, and 0.16 for compound **6**, respectively. This viscosity-dependent luminescence suggested that a viscous medium inhibited intramolecular rotation, thereby suppressing the nonradiative process which led to increased Φ_f. The λ_{em} of compound **3** showed almost no variation with changing solvent polarity, while compounds **4**, **5** and **6** showed a red shift of the λ_{em} with the increase of the polarity of solvents. This should be ascribed to ICT enhancement caused by the *N*,*N*-dimethylamino group in **D** ring.[6,7] Different from compounds **3**, **4** and **6**, the λ_{em} of compound **5** remained unchanged and only showed a red shift of the λ_{em} in ethylene glycol and glycerol. This difference may be explained by the inhibition of intramolecular rotation in ethylene glycol or glycerol which induced CT process in compound **5**.

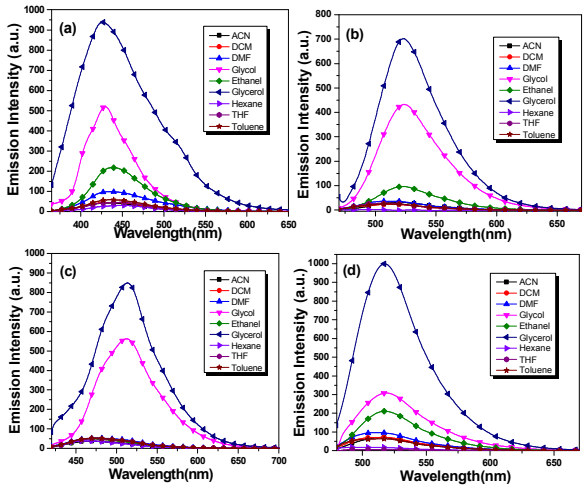

Fig. 2. Emission spectra of compounds **3** (a), **4** (b), **5** (c) and **6** (d) in various solvents such as hexane, toluene, dichloromethane (DCM), tetrahydrofuran (THF), acetonitrile (ACN), dimethylformamide (DMF), ethanol, ethylene glycol (glycol) and glycerol, respectively. λ_{ex}, 395 nm for **3**, 440 nm for **4**, 400 nm for **5**, and 450 nm for **6**.

In solid–state, compounds **3**–**6** showed their λ_{abs} and λ_{em} at 395 and 519 nm for compound **3**, 498 and 567 nm for compound **4**, 439 and 524 nm for compound **5**, 469 and 562 nm for compound **6**, respectively (Fig. S2 and Table 1). The red-shifted absorption bands (23–55 nm) and emission bands (51–70 nm) compared with those in THF should be ascribed to the increased intermolecular interactions and aggregation-induced

CT enhancement in their solid–state. Importantly, compounds **3**–**6** showed intense emission in solid–state, with Φ_f of 0.18 for compound **3**, 0.43 for compound **4**, 0.23 for compound **5**, and 0.14 for compound **6**, respectively (Fig. 3). The blocked intramolecular rotation due to the crystal matrix led to the luminescence enhancement in solid–state. All these confirmed that compounds **3**–**6** displayed the AIE nature in their aggregation state.

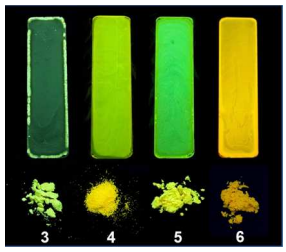

Fig. 3. The photo pictures of compounds **3**–**6** in drop-cast film and powder state (λ_{ex} = 365 nm using a UV lamp).

The AIE properties of compounds **3**–**6** were investigated in THF/water mixture of various ratios (Fig. 4 and Table 1). In pure THF, compounds **3**–**6** had very low emission intensity. When water was added to the THF solution, the emission intensity of compounds **3** and **5** kept almost the same until the water fraction (f_w) reached 70%. However, upon addition of 90% water in THF, the emission intensity of compounds **3** and **5** was significantly enhanced, and the Φ_f value was 0.06 for compound **3** and 0.07 for compound **5**, which was 11-fold higher than that in pure THF solution (Fig. S3). Interestingly, compounds **4** and **6** showed gradually increment of the emission intensity with the addition of water into THF solution. With f_w reached 90%, the Φ_f value was 0.07 for compound **4**, and 0.05 for compound **6**, which was 5- and 6-fold higher than that in pure THF solution (Fig. S3). A large red-shift of emission for compounds **3** (64 nm) and **5** (48 nm) was observed, while compounds **4** and **6** showed relatively small red-shift of emission (5 nm). Moreover, compounds **3**–**6** showed slightly red-shifted excitation band in THF/Water mixture (f_w =90%) when compared with those in THF, indicating their polarity-independent AIE behavior (Fig. S4). The aqueous solution of compounds **3**–**6** became turbid when the f_w exceeded 90%, respectively, because of the formation of visible aggregates that hindered the acquisition of the emission spectra. As mentioned above, the addition of water into the THF solutions of compounds **3**–**6** resulted in aggregation that led to enhanced emission. The restriction of phenyl rings free rotation via aggregates formation should be responsible for this AIE.[6]

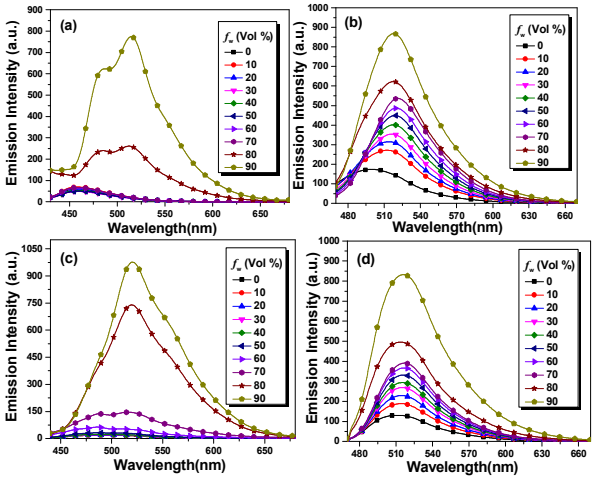

Fig. 4. Emission spectra of compounds **3** (a), **4** (b), **5** (c) and **6** (d) in THF/water mixtures (10 μM) with varied volumetric fractions of water (f_w). λ_{ex}, 395 nm for **3**, 440 nm for **4**, 400 nm for **5**, and 450 nm for **6**.

X-ray crystal structure analysis. To better understand the aggregation and solid-state emission properties, the molecular packing patterns of compounds **3**–**6** in the crystalline state were investigated. The ORTEP drawings and molecular packing structures of compounds **3**–**6** are shown in Fig. 5 and Fig. S5–8.

Compounds **3**–**6** belong to the orthorhombic space group *Pbca* for compound **3**, monoclinic space group *P*2(1)/*c* for compound **4**, monoclinic space group *P*2(1)/*c* for compound **5**, and monoclinic space group *C*2/*c* for compound **6**, respectively. All the boron atoms of compounds **3**–**6** adopt a typical tetrahedral geometry to form *N*^*O*–chelate six-membered rings (ring B), which contributes to the construction of the three-ring-fused π–conjugated skeletons. The bond lengths of B–N and B–O are 1.574(6) Å and 1.448(6) Å for compound **3**, 1.561(5) Å and 1.461(5) Å for compound **4**, 1.621(4) Å and 1.507(3) Å for compound **5**, and 1.617(4) Å and 1.508(3) Å for compound **6**, respectively. As anticipated, compounds **3**–**6** adopt propeller-shaped conformations. The dihedral angles of **B** and **C**, and **B** and **D** are 56.33° and 34.34° in compound **3**, 67.19° and 35.46° in compound **4**, 64.87° and 21.53° in compound **5**, 59.60° and 34.86° in compound **6**, respectively.

Journal Name RSCPublishing

ARTICLE

Table 1. Photophysical data of compounds **3**–**6** in solution and in solid-state.

Compound	In solution					In solid-state[f]		
	λ_{abs} (nm) ε (mol^{-1} cm^{-1}) THF [a]	λ_{em} (nm) (Φ_f) THF [a],[c]	λ_{em} (nm) (Φ_f) Aggr [b],[c]	λ_{em} (nm) (Φ_f) Glycerol [a], [c]	SS (cm^{-1}) [d]	λ_{abs} (nm)	λ_{em} (nm)	Φ_f [e]
3	372 (43000)	449 (<0.01)	513 (0.06)	449 (0.12)	4600	395	519	0.18
4	443 (49000)	512 (<0.01)	517 (0.07)	523 (0.26)	3000	498	567	0.43
5	404 (35000)	473 (<0.01)	521 (0.07)	513 (0.29)	3600	439	524	0.23
6	444 (43000)	510 (<0.01)	515 (0.05)	517 (0.16)	2900	469	562	0.14

[a] Measured at a concentration of 10 μM in THF or glycerol at 25 °C; [b] Measured at a concentration of 50 μM in THF/H_2O mixture with f_w of 90% at 25 °C; [c] Determined by using 4-methylamino-7-nitro-2,1,3-benzoxadiazole (Φ_f = 0.38 in acetonitrile) as reference; [d] Energy gap between the absorption and emission maxima; [e] Absolute quantum yield determined by calibrated integrating sphere systems; [f] Powder examples were used for the absorption and emission measurement.

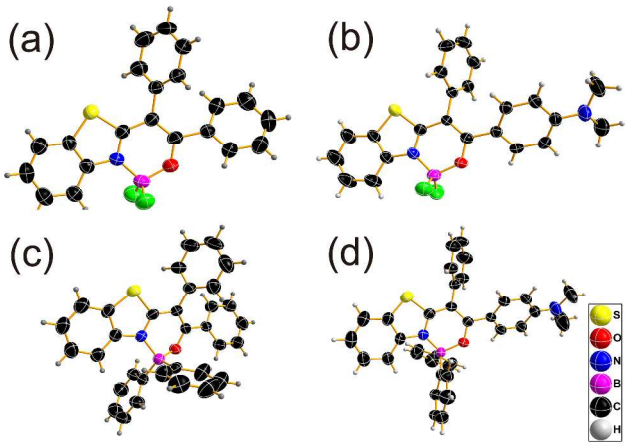

Fig. 5. Molecular structures of compounds **3** (a), **4** (b), **5** (c) and **6** (d) (50% probability for thermal ellipsoids).

None of intermolecular π–π interactions were detected in compounds **3**–**6**, while multiple short interatomic contacts existed within the crystals (Fig. S5–8): F1···H18–C18 (3.25 Å, 126.68°), F2···H2–C2 (3.30 Å, 140.03°), F2···H23–C23 (3.24 Å, 122.78°), F4···H14–C14 (3.47 Å, 150.04°), O1···H39–C39 (3.44 Å, 145.76°), B1 ··· H39–C39 (3.91 Å, 140.78°) interactions in compound **3**, F1···H6–C6 (3.17 Å, 133.64°), F2···H21–C21 (3.32 Å, 139.97°), S1–C13(3.49 Å), and S1···H19–C19 (3.49 Å, 116.60°) interactions in compound **4**, S1–C24 (3.14 Å) interactions in compound 5, and S1···H29–C29 (130.92°, 3.61 Å) interactions in compound **6**. Furthermore, C–H···π interactions were detected in compound **3** (3.35–3.98 Å), compound **4** (3.73 Å) and compound **6** (3.62 Å). These weak intermolecular interactions fix the molecular conformations of compounds **3**–**6** in solid-state, thus inhibiting the intramolecular rotations and blocking their non-radiative relaxation. These results agree well with the observation that compounds **3**–**6** showed intense emissions in solid-state.

Theoretical Calculations. The electronic structures and energy levels of compounds **3**–**6** were investigated by theoretical calculation. Time-dependent density functional theory (TD-DFT) at B3LYP with 6-31G(d,p) basis sets was used for calculation.[8] The pictorial drawings of HOMOs and LUMOs and energy levels are shown in Fig. 6.

Compounds **3** and **5** have HOMOs delocalized over the **A**, **B**, **C** and **D** rings, whereas their LUMOs are localized mainly on the orbitals from **A**, **B** and **D** rings. With *N*,*N*-dimethyl group in **D** ring, the HOMOs of compounds **4** and **6** are mainly delocalized over the **D** ring, and their LUMOs are localized mainly on the orbitals from **A** and **B** rings. A significant dense electron cloud is distributed on the **B** ring in the LUMOs of compounds **3**–**6**, due to the p_π–π* conjugation between p_π orbital of boron and π* orbitals of the aromatic rings, leading to low lying LUMO energy level. The calculated first excited state, mainly consisting of HOMO→LUMO transition, have excitation energies of 3.18 eV (390 nm, f = 0.5610) for compound **3**, 3.08 eV (403 nm, f = 0.8182) for compound **4**, 3.18 eV (390 nm, f = 0.3205) for compound **5**, and 2.97 eV (417 nm, f = 0.6400) for compound **6**, respectively, which are in good agreement with the experimental results in THF solution (Fig. S9). Due to the incorporation of *N*,*N*-dimethylamino group in **D** ring, the HOMOs and LUMOs of compounds **4** and **6** are destabilized and stabilized, respectively, relative to those of compounds **3** and **5**, thus decreasing the HOMO–LUMO gap, and resulting in red shift of the main absorption band relative to those of compound **3** and **5**. These results indicate that the main absorption bands of compounds **3**–**6** can be easily tuned, and that the extent of the shift of the absorption can be predicated by theoretical calculations.

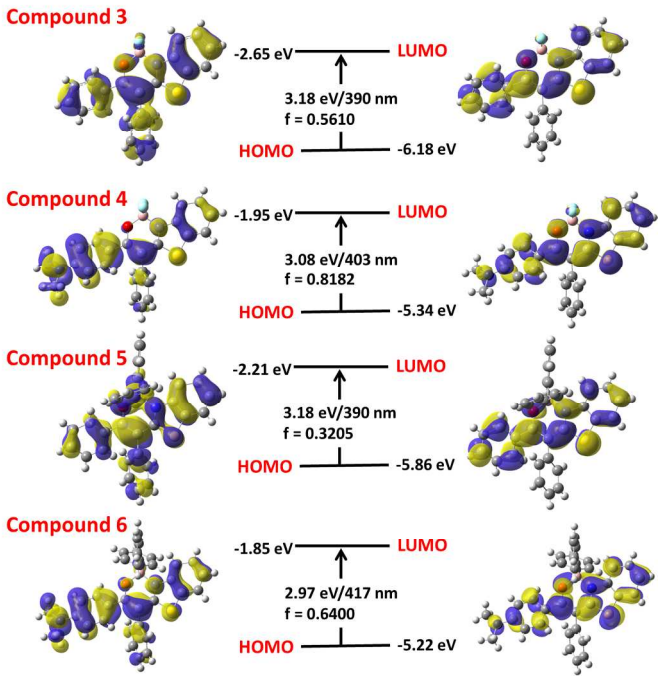

Fig 6. Moldecular orbital amplitude plots and energy levels of HOMOs and LUMOs of compounds **3**-**6** calculated by using B3LYP/6-31G(d, p) basis set with G03 Program.

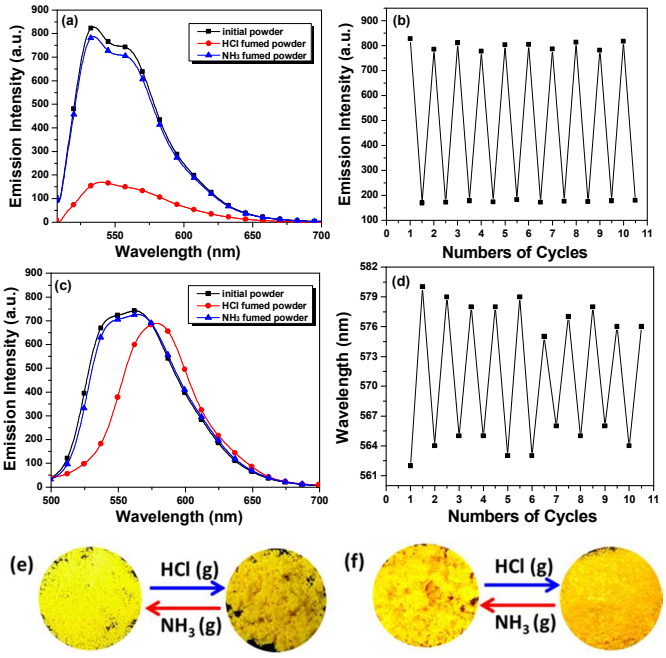

Fig. 7. Emission spectra of initial, HCl (g) and NH_3 (g) fumed powders of compound **4** (a) and compound **6** (c); (b) Reversible switching of the emission of compound **4** (b) and compound **6** (d) by HCl/NH_3 fuming cycle; λ_{ex}, 498 nm for **4**, and 469 nm for **6**. Luminescent pictures of HCl (g) and NH_3 (g) fumed powders of compound **4** (e) and compound **6** (f).

Acidochromic properties in solid-state. Compounds **4** and **6** possessed acidochromic behavior triggered by acid vapor since the *N,N*-dimethylamino group in compounds **4** and **6** can be easily protonated by acid, which holds the potential to develop into a kind of solid-state luminescence switching material (Fig. 7). When exposed to HCl vapors (37% concentrated hydrochloric acid vapors) for a few seconds, the luminescence of compound **4** was effectively quenched. This acid-induced emission quenching is probably because of the changed molecular conformation and packing structure in solid-state.[7b,9] Interestingly, compound **6** exhibited a red-shift of emission with colour changing from yellow to orange (562 nm to 580nm). The red-shift of the emission may be caused by the enhanced CT from benzothiazole moiety to the pronated *N,N*-dimethylamino group (Fig. S10). The protonated powder samples gradually recovered their original colour and luminescence when they were treated with NH_3 vapor (25% concentrated ammonium hydroxide vapors) for few minutes. The switching between emission red-shift/turn-on and emission blue-shift/quenching states by HCl/NH_3 vapor fuming can be carried out repeatedly (10 cycles) without obvious intensity decaying, demonstating the attractive luminescence switching properties of compound **4** and **6**.

Conclusions

In this article, four propeller-shaped organoboron complexes (**3**–**6**) derived from benzothiazole-enolate-based bidentate ligands were synthesized and characterized. These luminophores exhibited weak luminescence in low-viscosity organic solvents due to the intramolecular rotation induced nonradiative process. In high-viscosity organic solvents and aggregate state, these luminophores showed relatively strong luminescence, suggesting the intramolecular rotation induced nonradiative process was inhibited efficiently. Compounds **3**–**6** exhibited intense emission in solid-state with high quantum yield of 0.14-0.43. X–ray crystallographic analysis demonstrated that the weak intermolecular interactions such as F···H–C and C–H···π by fixing the molecular conformations of compounds **3**–**6** were responsible for intense luminescence in solid-state. Furthermore, compounds **4** and **6** were capable of sensing of acidic gas by reversible changes of emission, which may potentially serve as solid-state luminescent sensors for acidic vapors.

Experimental Section

General methods and materials

All the air-sensitive compound-involved reactions and manipulations were carried out in an atmosphere of dry argon by using Schlenk techniques and/or vacuum line techniques. Solvents were dried prior to use by the common methods in organometallic chemistry. Chemicals were commercially obtained and used as received. ^1H, and ^{13}C NMR spectra were recorded using Varian Mercury-plus 400M spectrometer. Chemical shifts were reported in ppm relative to $Si(CH_3)_4$ (^1H,

^{13}C), and coupling constants (*J*) were given in Hz. Mass spectra were obtained on a LCQ (ESI-MS, Thermo Finnigan) mass spectrometer. Column chromatography was performed using silica gel (200 mesh, Qingdao Haiyang Chemical Co., Ltd).

Synthesis

General procedure for the synthesis of compounds 1 and 2. 2-benzyl-benzothiazole (1 equiv.) was added to a mixture of THF and NaH (60w% in oil, 5 equiv.) at room temperature, after stirred for 20 minutes, methyl benzoate or methyl 4-(dimethylamino) benzonate (1 equiv.) was added, and the resulting mixture was heated at reflux for 10 h. After cooling to room temperature, 2 M HCl aq. was slowly added, and the yellow precipitate was filtered and washed with water. After drying, the desire product was obtained as yellow solid.

Compound 1a and **1b** was obtained (**1a**: **1b** = 1: 2); Yield: 90%, ^{1}H NMR (400 MHz, $CDCl_3$): δ/ppm = 8.07 (d, J = 7.9 Hz, 2H), 8.00 (d, J = 8.1 Hz, 1H), 7.88–7.83 (m, 6H), 7.70 (d, J = 7.9 Hz, 3H), 7.54 (d, J = 7.1 Hz, 3H), 7.45 (dd, J = 12.9, 7.1 Hz, 7H), 7.41–7.09 (m, 42H), 6.60 (s, 1H).

Compound 2 Yield: 92%, ^{1}H NMR (400 MHz, $CDCl_3$): δ/ppm = 8.03 (d, J = 8.2 Hz, 1H), 7.62 (d, J = 7.9 Hz, 1H), 7.42 (t, J = 7.8 Hz, 1H), 7.31–7.17 (m, 5H), 7.12 (d, J = 8.9 Hz, 3H), 6.46 (d, J = 8.8 Hz, 2H), 5.87 (s, 1H), 2.92 (s, 6H). ^{13}C NMR (100 MHz, $CDCl_3$): δ/ppm =163.8, 161.7, 150.8, 143.6, 143.1, 130.6, 128.7, 128.4, 128.2, 127.7, 127.4, 125.7, 124.4, 123.3, 121.5, 117.7, 111.1, 40.1.

General procedure for the synthesis of compounds 3 and 4. Compounds **1** and **2** (1 equiv.) were dissolved in dry toluene. DBU (3 equiv.) was added to the solution and stirred for 10 minutes at room temperature. A solution of toluene containing of boron trifluoride diethyl ether complex (5 equiv.) was slowly added to the mixture via syringe. The mixture was heated to reflux for 2 h. Then the solution was cooled to room temperature and poured into water. The organic phase was extracted with dichloromethane. The organic layer was dried over magnesium sulfate and the solvent was removed under vacuum. Pure product was then obtained by silica gel column chromatography.

Compounds 3 Yield: 72%, R_f = 0.3 (petroleum ether: dichloromethane = 3: 1), ^{1}H NMR (400 MHz, $CDCl_3$) δ/ppm = 8.24 (d, J = 8.7 Hz, 1H), 7.69 (d, J = 8.0 Hz, 1H), 7.60 (t, J = 7.8 Hz, 1H), 7.51–7.38 (m, 6H), 7.38–7.28 (m, 3H), 7.20 (t, J = 7.7 Hz, 2H). ^{13}C NMR (100 MHz, $CDCl_3$) δ/ppm = 172.5, 163.9, 143.4, 135.2, 134.3, 131.3, 130.7, 130.1, 130.1, 129.5, 128.3, 127.9, 126.0, 121.7, 119.0, 106.9. HRMS (ESI): calcd., $[M+Na]^+$ = 400.0753, found: $[M+Na]^+$ = 400.0776.

Compounds 4 Yield: 43%, R_f = 0.3 (petroleum ether: dichloromethane = 3: 1), ^{1}H NMR (400 MHz, $CDCl_3$) δ/ppm = 8.14 (d, J = 8.3 Hz, 1H), 7.59 (d, J = 8.0 Hz, 1H), 7.52 (t, J = 7.8 Hz, 1H), 7.49–7.43 (m, 3H), 7.42–7.34 (m, 4H), 7.32 (d, J = 7.4 Hz, 1H), 6.42 (d, J = 9.1 Hz, 2H), 2.95 (s, 6H). ^{13}C NMR (100 MHz, $CDCl_3$) δ/ppm = 172.2, 164.2, 152.0, 143.7, 136.5, 132.1, 131.6, 129.9, 128.8, 128.0, 125.2, 121.4, 120.7, 118.4, 110.6, 104.7, 40.0. HRMS (ESI): calcd., $[M]^+$ = 421.1356, found: $[M]^+$ = 421.1383, $[M+Na]^+$ =443.1194.

General procedure for the synthesis of compounds 5 and 6. Compounds **1** and **2** (1 equiv.) were dissolved in dry toluene, triphenylboron (1 equiv.) was added to the solution and the resulting mixture was heated to reflux for 3 h. The solvent was removed under vacuum after cooling to room temperature. Pure product was then obtained by silica gel column chromatography.

Compounds 5 Yield: 78%, R_f = 0.3 (petroleum ether: ethyl acetate= 10: 1), ^{1}HNMR (400 MHz, $CDCl_3$) δ/ppm = 7.61 (d, J = 7.9 Hz, 1H), 7.47 (dd, J = 7.2, 1.9 Hz, 4H), 7.41 (d, J = 7.3 Hz, 2H), 7.39–7.34 (m, 3H), 7.25 (ddd, J = 15.1, 7.2, 4.0 Hz, 10H), 7.12 (dd, J = 9.6, 5.0 Hz, 4H). ^{13}C NMR (100 MHz, $CDCl_3$) δ/ppm = 172.2, 166.4, 145.9, 136.6, 135.5, 133.5, 131.8, 130.0, 129.4, 128.6, 127.7, 127.3, 126.7, 124.6, 121.4, 119.9, 107.5. HRMS (ESI): calcd., $[M+Na]^+$ = 516.1570, found: $[M+Na]^+$ = 516.1600.

Compounds 6 Yield: 75% R_f = 0.3 (petroleum ether: dichloromethane = 3: 1), ^{1}H NMR (400 MHz, $CDCl_3$) δ/ppm = 7.55 (d, J = 8.1 Hz, 1H), 7.49 (d, J = 6.6 Hz, 4H), 7.40 (d, J = 6.5 Hz, 4H), 7.37 (s, 1H), 7.31 (d, J = 7.4 Hz, 2H), 7.26 (s, 5H), 7.15 (dd, J = 14.2, 6.6 Hz, 1H), 7.09 (d, J = 7.4 Hz, 2H), 7.05 (d, J = 8.3 Hz, 1H), 6.39 (d, J = 8.9 Hz, 2H), 2.92 (s, 6H). ^{13}C NMR (100 MHz, $CDCl_3$) δ/ppm = 171.8, 166.4, 151.7, 146.1, 137.8, 133.5, 132.1, 131.9, 129.5, 128.3, 127.2, 126.9, 126.50, 123.9, 122.1, 121.2, 119.2, 110.6, 105.7, 40.0. HRMS (ESI): calcd., $[M+Na]^+$ = 559.1992, found: $[M+Na]^+$ = 559.2010.

Spectroscopic measurements

UV-vis absorption spectra were recorded on a Shimadzu UV-3600 spectrometer with a resolution of 1.0 nm. A solution of the sample (ca. 10^{-5} M) in a 1 cm square quarts cell was used for the measurement. Luminescence spectra were recorded on a Hitachi F-7000 spectrometer. The luminescence lifetimes and the absolute quantum yields (Φ_f) of the samples were determined with a Horiba Jobin Yvon Fluorolog-3 spectrofluorimeter. Luminescence quantum yield of compounds **3**–**6** in solution were determined by using 4-methylamino-7-nitro-2,1,3-benzoxadiazole (Φ_f = 0.38 in acetonitrile) as reference.[10]

X-ray structure determination

The X-ray diffraction data were collected at 298 K on a Gemini A Single Crystal CCD X-ray diffractometer with $Mo_{K\alpha}$ radiation (l = 0.71073 Å) and graphite monochromator. The structure was solved by direct methods (SHELX-97)[11] and refined by the full-matrix least-squares on F_2 (SHELX-97). All the non-hydrogen atoms were refined anisotropically and all the hydrogen atoms were placed by using AFIX instructions.

Compound 3 $C_{21}H_{14}BF_2NOS$; M = 377.20, Orthorhombic, a = 13.5821(13) Å, b = 17.5606(15) Å, c = 33.639(3) Å, α = 90.00°, β = 90.00°, γ = 90.00°, V = 8023.2(12) Å^3, T = 298(2) K, space group *Pbca*, Z = 16, 30914 reflections measured, 7061 independent reflections (R_{int} = 0.1397). The final R_1 values were 0.0527 ($I > 2\sigma(I)$). The final w$R(F^2)$ values were 0.0999 ($I > 2\sigma(I)$). GOF = 0.750. CCDC 1059226.

Compound 4 $C_{23}H_{19}BF_2N_2OS$; M = 420.27, Monoclinic, a = 12.4688(11) Å, b = 11.0347(9) Å, c = 14.9694(12) Å, α =

90.00°, β = 90.2580 (10)°, γ = 90.00°, V = 2059.6(3) Å^3, T = 298(2) K, space group $P2(1)/c$, Z = 4, 10131 reflections measured, 3630 independent reflections (R_{int} = 0.0720). The final R_1 values were 0.0535 ($I > 2\sigma(I)$). The final w$R(F^2)$ values were 0.1106 ($I > 2\sigma(I)$). GOF = 0.951. CCDC 1059227.

Compound 5 $C_{31}H_{24}BFNOS$; M = 493.40, Monoclinic, a = 10.9909(8) Å, b = 9.0950(7) Å, c = 26.758(2) Å, α = 90.00°, β = 99.025(2)°, γ = 90.00°, V = 2641.7(3) Å^3, T = 298(2) K, space group $P2(1)/c$, Z = 4, 13002 reflections measured, 4649 independent reflections (R_{int} = 0.0856). The final R_1 values were 0.0484 ($I > 2\sigma(I)$). The final w$R(F^2)$ values were 0.0945 ($I > 2\sigma(I)$). GOF = 0.724. CCDC 1059228.

Compound 6 $C_{35}H_{29}BN_2OS$; M = 420.27, Monoclinic, a = 30.53(3) Å, b = 12.606(11) Å, c = 16.241(15) Å, α = 90.00°, β = 111.74(2)°, γ = 90.00°, V = 5806(10) Å^3, T = 298(2) K, space group $C2/c$, Z = 8, 14581 reflections measured, 5125 independent reflections (R_{int} = 0.0843). The final R_1 values were 0.0529 ($I > 2\sigma(I)$). The final w$R(F^2)$ values were 0.1069 ($I > 2\sigma(I)$). GOF = 0.809. CCDC 1059229.

Computational details

TD-DFT calculations were performed at the hybrid density functional theory level (B3LYP) with the 6-31G(d,p) basis set, using the Gaussian03 software package. The calculations were made in the gas phase.[8]

Acknowledgements

We thank the Natural Science Foundation of China (nos. 21301085), the Natural Science Foundation of Shandong Province (ZR2011BQ010), and the Liaocheng University Funds for Young Scientists (31805) for financial support.

Notes and references

[a] Institute of Functional Organic Molecules and Materials, School of Chemistry and Chemical Engineering, Liaocheng University, No.1 Hunan Road, Liaocheng, 252000, People's Republic of China; E-mail: chliuzp@163.com; wangxiaoqing@lcu.edu.cn.

[b] School of Material Science and Engineering, Liaocheng University, No.1 Hunan Road, Liaocheng, 252000, People's Republic of China;

[c]. State Key Laboratory of Coordination Chemistry, Coordination Chemistry Institute, School of Chemistry and Chemical Engineering, Nanjing University, Nanjing, P.R. China, 210093. E-mail: heweij69@nju.edu.cn.

†Both authors contribute equally to this work.

Electronic Supplementary Information (ESI) available: Synthesis, ^{1}H, ^{13}C, NMR spectra, absorption and luminescent spectra of compounds **3-6**. See DOI: 10.1039/b000000x/

1 (a) N. Boens, V. Leen, W. Dehan, *Chem. Soc. Rev.*, 2012, **41**, 1130; (b) T. Bura, N. Leclerc, S. Fall, P. Léveque, T. Heiser, P. Retailleau, S. Rihn, A. Mirloup, R. Ziessel, *J. Am. Chem. Soc.*, 2012, **134**, 17404.

2 (a) A. Loudet, K. Burgess, *Chem. Rev.,* 2007, **107**, 4891; (b) G. Ulrich, R. Ziessel, A. Harriman, *Angew. Chem. Int. Ed.,* 2008, **47**, 1184; (c) D. Frath, J. Massue, G. Ulrich, and R. Ziessel, *Angew. Chem., Int. Ed.*, 2014, **53**, 2290; (d) H. Lu, J. Mack, Y. Yang, Z. Shen, *Chem. Soc. Rev.*, 2014, **43**, 4778.

3 (a) A. Hepp, G. Uirich, R. Schmechel, H. von Seggern, R. Ziessel, *Synth. Met*., 2004, **146**, 11; (b) D. Zhang, Y. Wen, Y. Xiao, G. Yu, Y. Liu, X. Qian, *Chem. Commun*., 2008, 4777; (c) T. Ozdemir, S. Atilgan, I. Kutuk, L. T. Yildirim, A. Tulek, M. Bayindir, E. U. Akkaya, *Org. Lett*., 2009, **11**, 2105.

4 (a) H. Lu, Q. Wang, L. Gai, Z. Li, Y. Deng, X. Xiao, G. Lai and Z. Shen, *Chem. –Eur. J*., 2012, **18**, 7852; (b) L. Gai, H. Lu, B. Zou, G. Lai, Z. Shen, Z. Li, *RSC Advances*., 2012, **2**, 8840; (c) G.-L. Fu, H. Pan, Y.-H. Zhao, C.-H. Zhao, *Org. Biomol. Chem*., 2011, **9**, 8141. (d) Y. Kubota, J. Uehara, K. Funabiki, M. Ebihara, M. Matsui, *Tetrahedron Lett*., 2010, **51**, 6195; (e) T. T. Vu, S. Badré, C. Dumas-Verdes, J. J.Vachon, C. Julien, P. Audebert, E. Y. Senotrusova, E. Y. Schmidt, B. A. Trofimov, R. B. Pansu, G. Clavier, R. Méallet-Renault, *J. Phys. Chem. C*., 2009, **113**, 11844.

5 (a) Y. Yang, X. Su, C. N. Carroll, I. Aprahamian, *Chem. Sci*., 2012, **3**, 610; (b) Y. Zhou, J. W. Kim, R. Nandhakumar, M. J. Kim, E. Cho, Y. S. Kim, Y. H. Jang, C. Lee, S. Han, K. M. Kim, J.-J. Kim, J. Yoon, *Chem. Common*., 2010, **46**, 6512; (c) J. F. Araneda, W. E. Piers, B. Heyne, M. Parvez, R. McDonald, *Angew. Chem. Int. Ed*., 2011, **50**, 12214; (d) R. Yoshii, A. Hirose, K. Tanaka, Y. Chujo, *Chem. –Eur. J*., 2014, **20**, 8320; (e) H. Liu, H. Lu, J. Xu, Z. Liu, Z. Li, J. Mack, Z. Shen, *Chem. Common*., 2014, **50**, 1074; (f) K. Benelhadj, J. Massue, P. Retailleau, G. Ulrich, R. Ziessel, *Org. Lett*., 2013, **15**, 2918; (g) Y.-Y. Wu, Y. Chen, G.-Z. Gou, W.-H. Mu, X.-J. Lv, M.-L. Du, W.-F. Fu, *Org. Lett.*, 2012, **14**, 5226; (h) D. Frath, A. Poirel, G. Ulrich, A. D. Nicola, R. Ziessel, *Chem. Commun*., 2013, **49**, 4908; (i) S. Shimizu, T. Lino, Y. Araki, N. *Chem. Commun*., 2013, **49**, 1621; (j) Y. Ni, W. Zeng, K.-W. Huang, J. Wu, *Chem. Commun*., 2013, **49**, 1217; (k) H. Liu, H. Lu, F. Wu, Z. Li, N. Kobayashi, Z. Shen, *Org. Biomol. Chem*., 2014, **12**, 8223; (l) N. Gao, C. Cheng, H. Yu, E. Hao, S. Wang, J. Wang, Y. Wei, X. Mu, L. Jiao, *Dalton Trans*., 2014, **43**, 7121; (m) H. Liu, H. Lu, Z. Zhou, S. Shimizu, Z. Li, N. Kobayashi, Z. Shen, *Chem. Commun*., 2015, **51**, 1713; (n) R. S. Singh, M. Yadav, R. K. Gupta, R. Pandey and D. S. Pandey, *Dalton Trans*., 2013, **42**, 1696.

6 (a) Y. Hong, J. W. Y. Lam, B. Z. Tang, *Chem. Commun*., 2009, 4332; (b) Y. Hong, J. W. Y. Lam, B. Z. Tang, *Chem. Soc. Rev*., 2011, **40**, 5361; (c) Z. Zhao, J. W. Y. Lam, B. Z. Tang, Curr. *Org. Chem*., 2010, **14**, 2109. (d) J. Luo, Z. Xie, J. W. Y. Lam, L. Cheng, H. Chen, C. Qiu, H. S. Kwok, X. Zhan, Y. Liu, D. Zhu, B. Z. Tang, *Chem. Commun*., 2001, 1740. (e) Q. Zeng, Z. Li, Y. Dong, C. Di, A. Q in, Y. Hong, L. Ji, Z. Zhu, C. K. W. Jim, G. Yu, Q. Li, Z. Li, Y. Liu, J. Qin, B. Z. Tang, *Chem. Commun*., 2007, 70. (f) Z. Zhao, Z. Wang, P. Lu, C. Y. K. Chan, D. Liu, J. W. Y. Lam, H. H. Y. Sung, I. D. Williams, Y. Ma, B. Z. Tang, *Angew. Chem. Int. Ed.,* 2009, **48**, 7608. (g) W. Z. Yuan, P. Lu, S. Chen, J. W. Y. Lam, Z. Wang, Y. Liu, H. S. Kwok, Y. Ma, B. Z. Tang, *Adv. Mater*., 2010, **22**, 2159. (h) B.-K. An, S.-K. Kwon, S.-D. Jung, S. Y. Park, *J. Am. Chem. Soc.,* 2002, **124**, 14410. (i) Z. Yang, Z. Chi, T. Yu, X. Zhang, M. Chen, B. Xu, S. Liu, Y. Zhang, J. Xu, *J. Mater. Chem*., 2009, **19**, 5541. (j) R. Deans, J. Kim, M. R. Machacek, T. M. Swager, *J. Am. Chem. Soc*., 2000, 122, 8565. (k) F. Würthner, T. E. Kaiser, C. R. Saha-Möller, A*ngew. Chem. Int. Ed.* 2011, **50**, 3376. (l) K. Tanabe, D. Kodama, M. Hasegawa, T. Kato, *Chem. Lett*., 2014, **43**, 186.

7 (a) X. Wang, Y. Wu, Z. Li, Q. Liu, H. Yan, C. Ji, J. Duan, Z. Liu, *Chem. Common.,* 2015, **51**, 784. (b) X. Wang, Q. Liu, H. Yan, Z. Liu,

M. Yao, Q. Zhang, S. Gong, W. He, *Chem. Common.,* 2015, **51**, 7497. (c) Q. Liu, X. Wang, H. Yan, Y. Wu, Z. Li, S. Gong, P. Liu, Z. Liu, *J. Mater. Chem. C*., 2015, **3**, 2953. (d) Y. Wu, Z. Li, Q. Liu, X. Wang, H. Yan, S. Gong, Z. Liu, W. He, *Org.& Biomole. Chem.,* 2015, **13**, 5775. (e) X. Wang, H. Liu, J. Cui, Y. Wu, H. Lu, J. Lu, Z. Liu and W. He, *New J. Chem*., 2014, **38**, 1277.

8 Gaussian 03, Revision B. 05, M. J. Frisch, G. W. Trucks, H. B. Schlegel, G. E. Scuseria, M. A. Robb, J. R. Cheeseman, J. A. Montgomery, Jr., T. Vreven, K. N. Kudin, J. C. Burant, J. M. Millam, S. S. Iyengar, J. Tomasi, V. Barone, B. Mennucci, M. Cossi, G. Scalmani, N. Rega, G. A. Petersson, H. Nakatsuji, M. Hada, M. Ehara, K. Toyota, R. Fukuda, J. Hasegawa, M. Ishida, T. Nakajima, Y. Honda, O. Kitao, H. Nakai, M. Klene, X. Li, J. E. Knox, H. P. Hratchian, J. B. Cross, V. Bakken, C. Adamo, J. Jaramillo, R. Gomperts, R. E. Stratmann, O. Yazyev, A. J. Austin, R. Cammi, C. Pomelli, J. W. Ochterski, P. Y. Ayala, K. Morokuma, G. A. Voth, P. Salvador, J. J. Dannenberg, V. G. Zakrzewski, S. Dapprich, A. D. Daniels, M. C. Strain, O. Farkas, D. K. Malick, A. D. Rabuck, K. Raghavachari, J. B. Foresman, J. V. Ortiz, Q. Cui, A. G. Baboul, S. Clifford, J. Cioslowski, B. B. Stefanov, G. Liu, A. Liashenko, P. Piskorz, I. Komaromi, R. L. Martin, D. J. Fox, T. Keith, M. A. Al-Laham, C. Y. Peng, A. Nanayakkara, M. Challacombe, P. M. W. Gill, B. Johnson, W. Chen, M. W. Wong, C. Gonzalez, and J. A. Pople, Gaussian, Inc., Pittsburgh, PA, **2003**.

9 X. Chen, Z. Zhang, H. Zhang, S. Han, K. Ye, L. Wang, H. Zhang, and Y. Wang, *J. Mater. Chem. C*., 2014, **2**, 7385.

10 Uchiyama, S.; Matsumura, Y.; de Silva, A. P.; Iwai, K. *Anal. Chem*., 2003, **75**, 5926.

11 Sheldrick, G. M. *SHELX-97*, *Program for the Refinement of Crystal Structures*;University of Göttingen: Göttingen, Germany, 199**7**

GRAPHIC ABSTRACT

Four benzothiazole-ketoiminate-based organoboron complexes were demonstrated to possess aggregation-induced emission, large Stokes shift and high quantum yield in the solid-state, which were rationalized through X-ray crystal analysis, and electronic structure calculations.